

Second harmonic generation in glass-based metasurfaces using tailored surface lattice resonances

Tapajyoti Das Gupta[†], Louis Martin-monier[†], Jeremy Butet^{††}, Kuang-Yu Yang^{††}, Andreas Leber[†], Chaoqun Dong[†], Tung Nguyen-Dang[†], Wei Yan[†], Olivier J.F. Martin^{††}, Fabien Sorin

*†**

*†*Photonic Materials and Fiber Devices Laboratory, Institute of Materials, Ecole Polytechnique Fédérale de Lausanne (EPFL), Lausanne, Switzerland.

*††*Nanophotonics and Metrology Laboratory, École Polytechnique Fédérale de Lausanne (EPFL), 1015 Lausanne, Switzerland

1. Sample Fabrication process

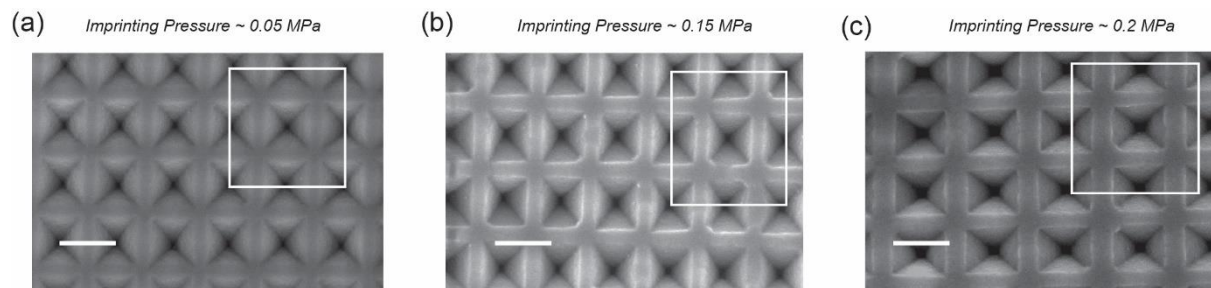


Figure S.I.1. SEM image illustrating the effect of applied pressure during nanoimprinting (a) period 360 nm (applied Pressure 0.05 MPa) (b) period 400 nm (applied pressure 0.015MPa) (c) period 480 nm (applied pressure 0.2MPa) . Scale Bar 350 nm.

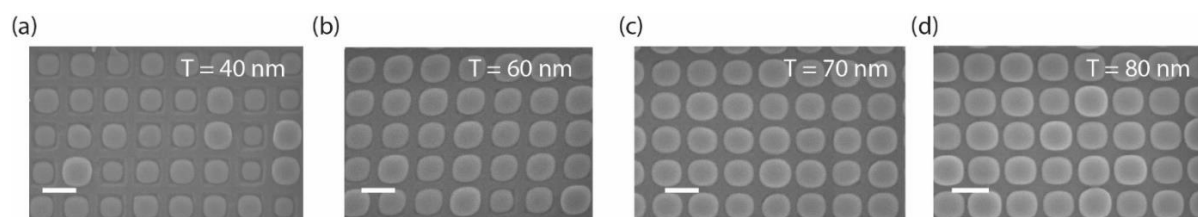


Figure S.I.2. Successive dewetting process. SEM images (a) to (d) illustrating that by the process of successive dewetting (deposition and dewetting of successive thin films) the inter-particle gap and particle size can be tuned. Inset shows the total deposited thickness of the film.

2. Optical constant of Selenium

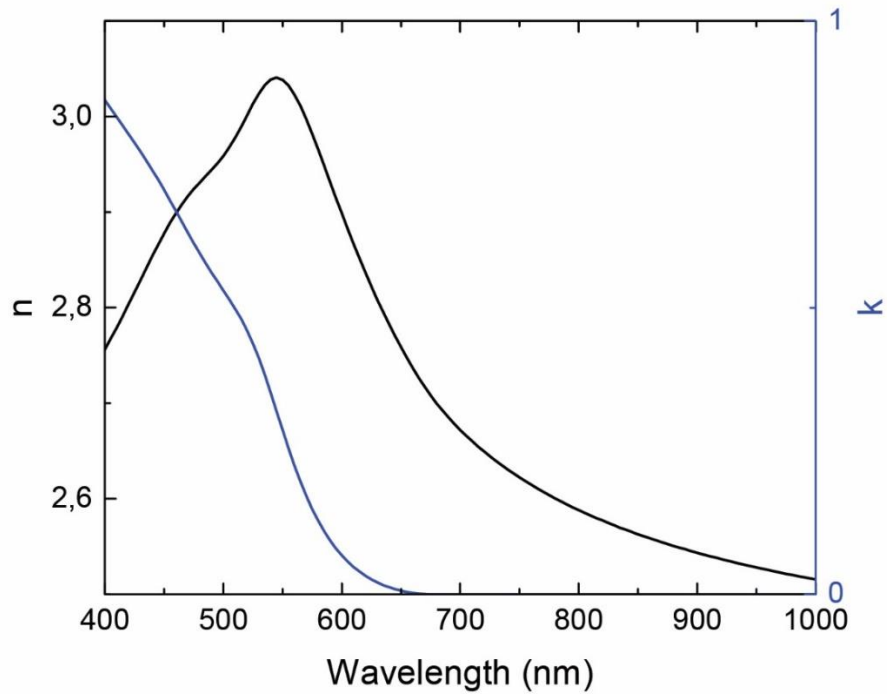


Figure S.I.3. Optical constant of Selenium obtained by ellipsometry

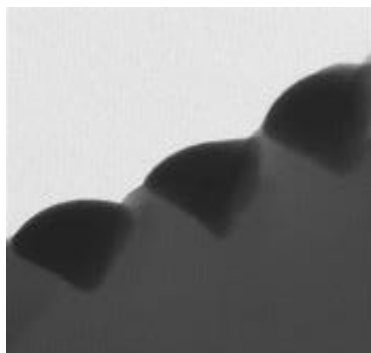


Figure S.I.4: Bright field TEM image showing the conical structure of the particle

3. Single particle scattering analysis

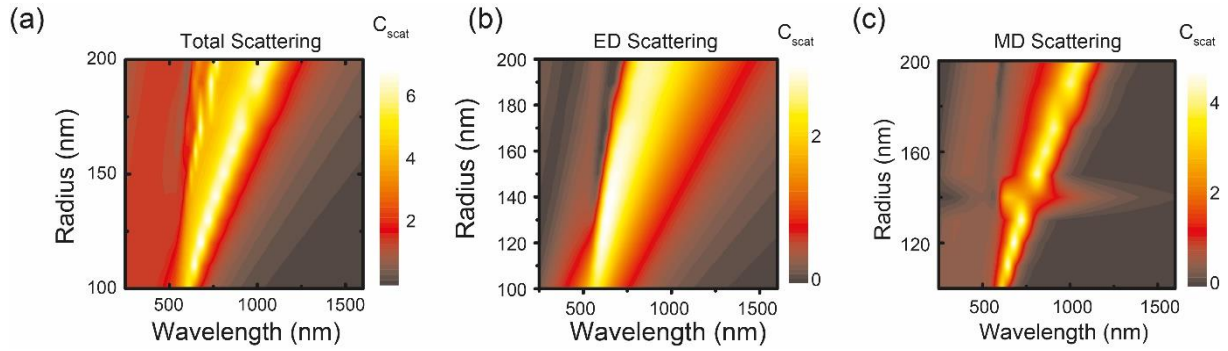


Figure S.I.5. Single particle numerical analysis as a function of radius (a) multipole expansion of scattering spectra (b) electric dipole (c) magnetic dipole evaluated with Mie theory for Selenium (Se).

Mie theory was used to calculate the single particle scattering cross-section. Scattering cross-section of a single homogeneous sphere is given by:

$$C_{scat} = \frac{2\pi}{k^2} \sum_n (|a_n|^2 + |b_n|^2)$$

Where k is the wavenumber, a_n , b_n are the n th order of electric and magnetic Mie coefficients respectively; and $n=1$ and 2 indicates the dipole and quadruple moments respectively. Figure 1(a) shows the calculated C_{scat} as a function of particle radius and wavelength, revealing a red-shift for both the electric dipole (ED) and the magnetic dipole (MD) resonance. In a sharp contrast to the broad ED, MD exhibits a narrower linewidth with a larger contribution to the total extinction cross-section than the ED resonance. The main contribution of the scattering spectra thus comes from the MD for larger particle size. Importantly, both the ED and MD resonances lie above the lossless region of the bulk selenium for a particle size of 300 nm, satisfying design criteria.

4. Field profile distribution at critical coupling:

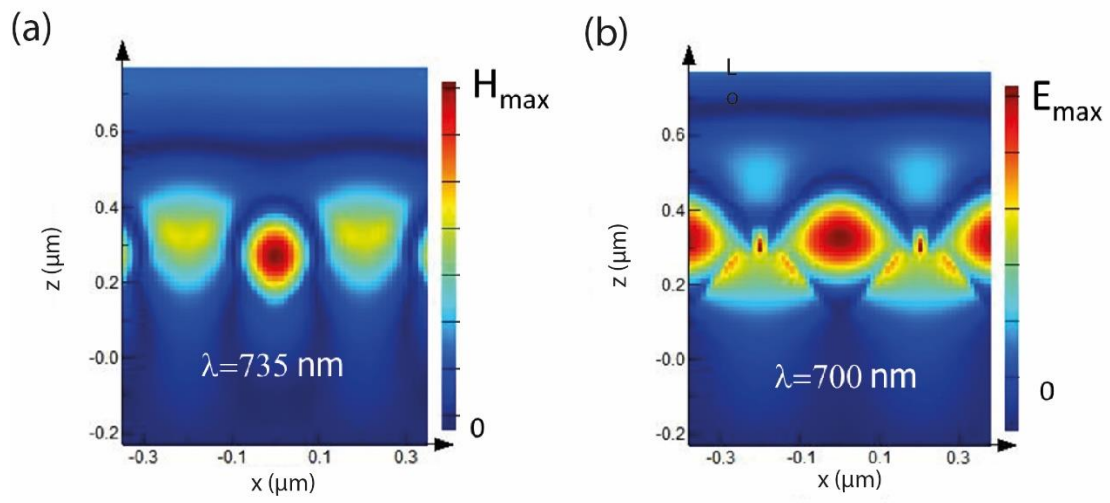


Figure S.I.6. (a) Magnetic and (b) electric plot at their corresponding resonance for a 400 nm period.

5. Effect of mode coupling by lattice tuning:

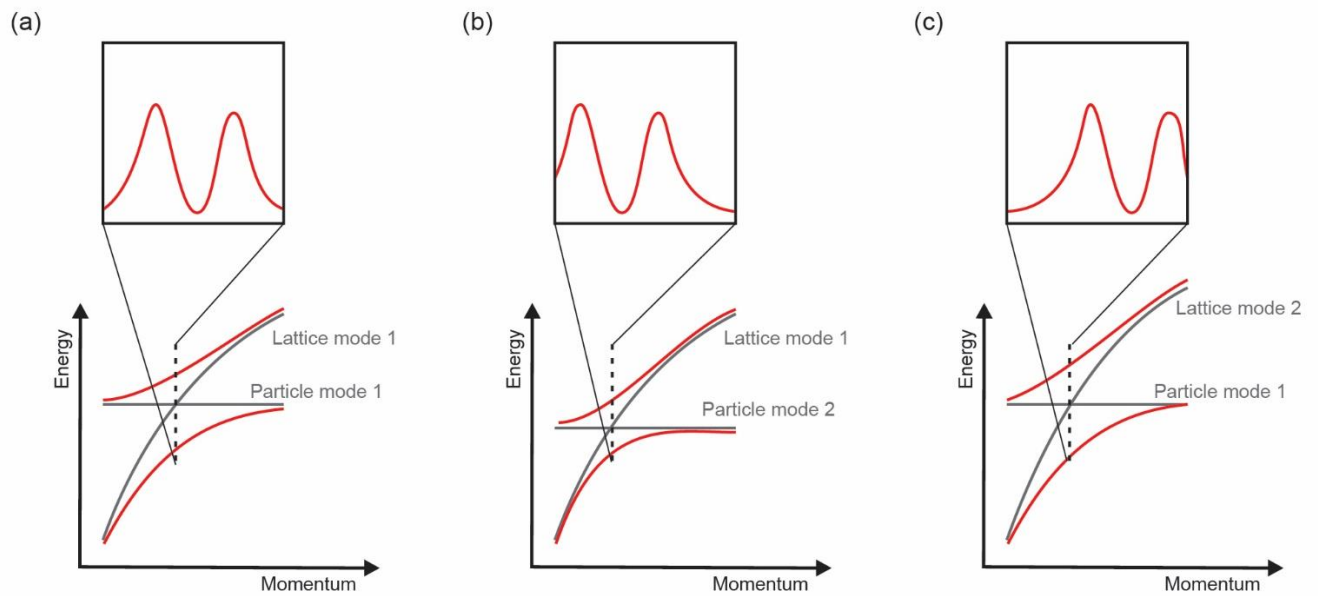


Figure S.I.7. Schematic illustration of mode coupling and mode movement

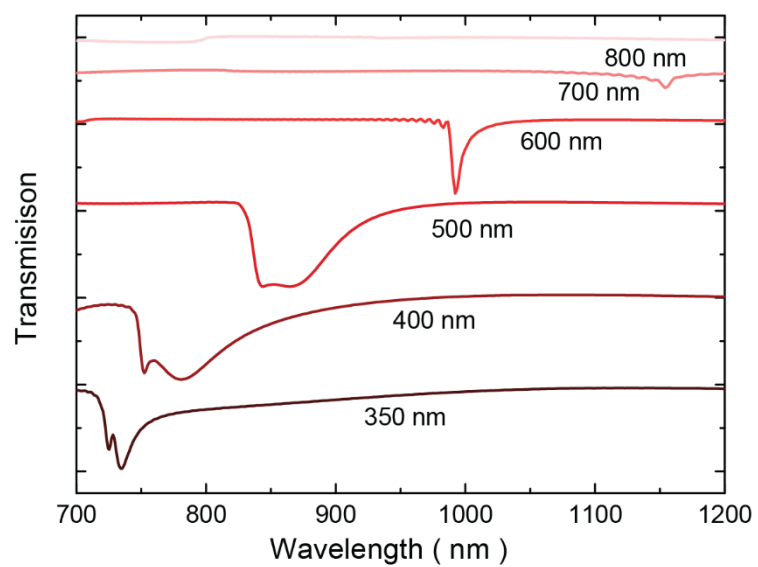


Figure S.I.8. Simulation of transmission illustrating the dip positions with increasing periodicities

6. Power law dependency of SHG

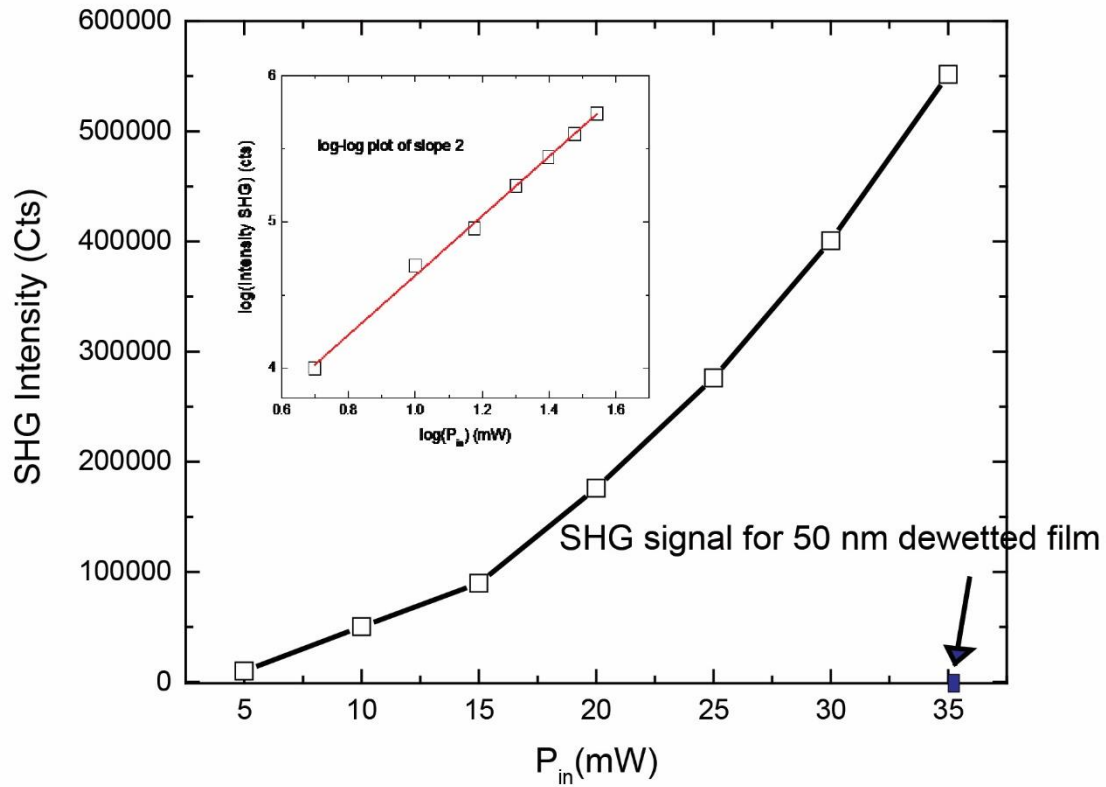


Figure S.I.9. Power law dependency of the emitted signal at 400 nm when the fundamental wavelength is 800 nm. Inset shows the log-log plot of the curve showing a linear fit of slope 2. SHG intensity of the metasurface due to fundamental field enhancement is at least 4 orders of magnitude higher than the thin film (below 1000 cts at 35mW power) indicated with blue dot.

7. SHG Spectrum at Resonant and non resonant region

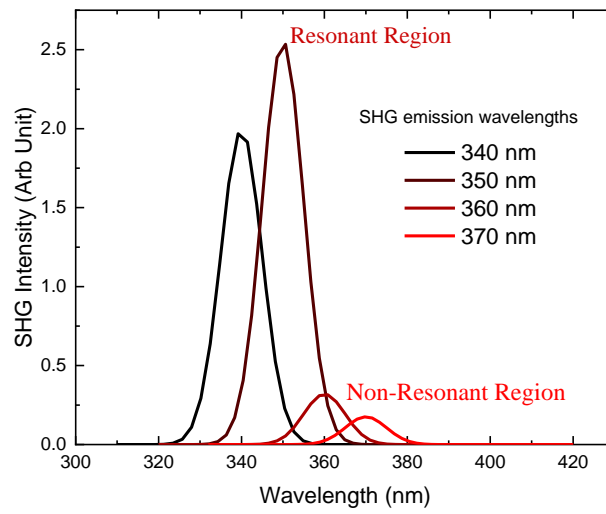


Figure S.I.10. SHG emitted spectrum at resonant and non-resonant region

8. Polarization dependency of emitted SHG

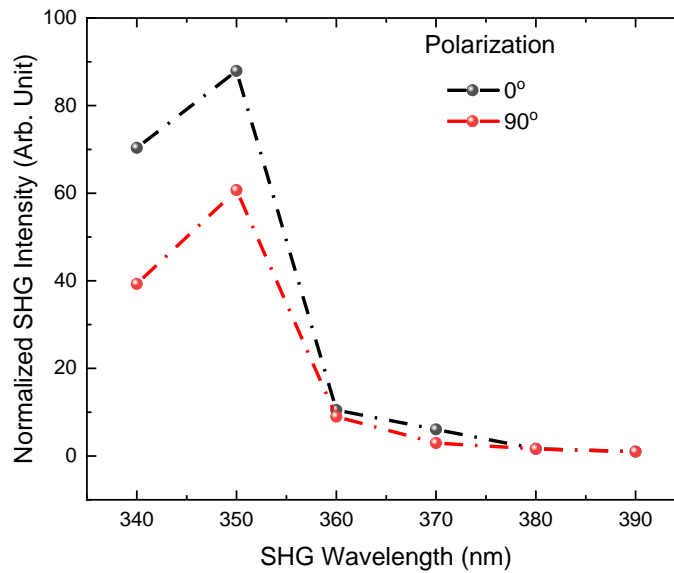


Figure S.I.11. Polarization dependency of SHG emission

9. Quadratic dependency of the Field enhancement:

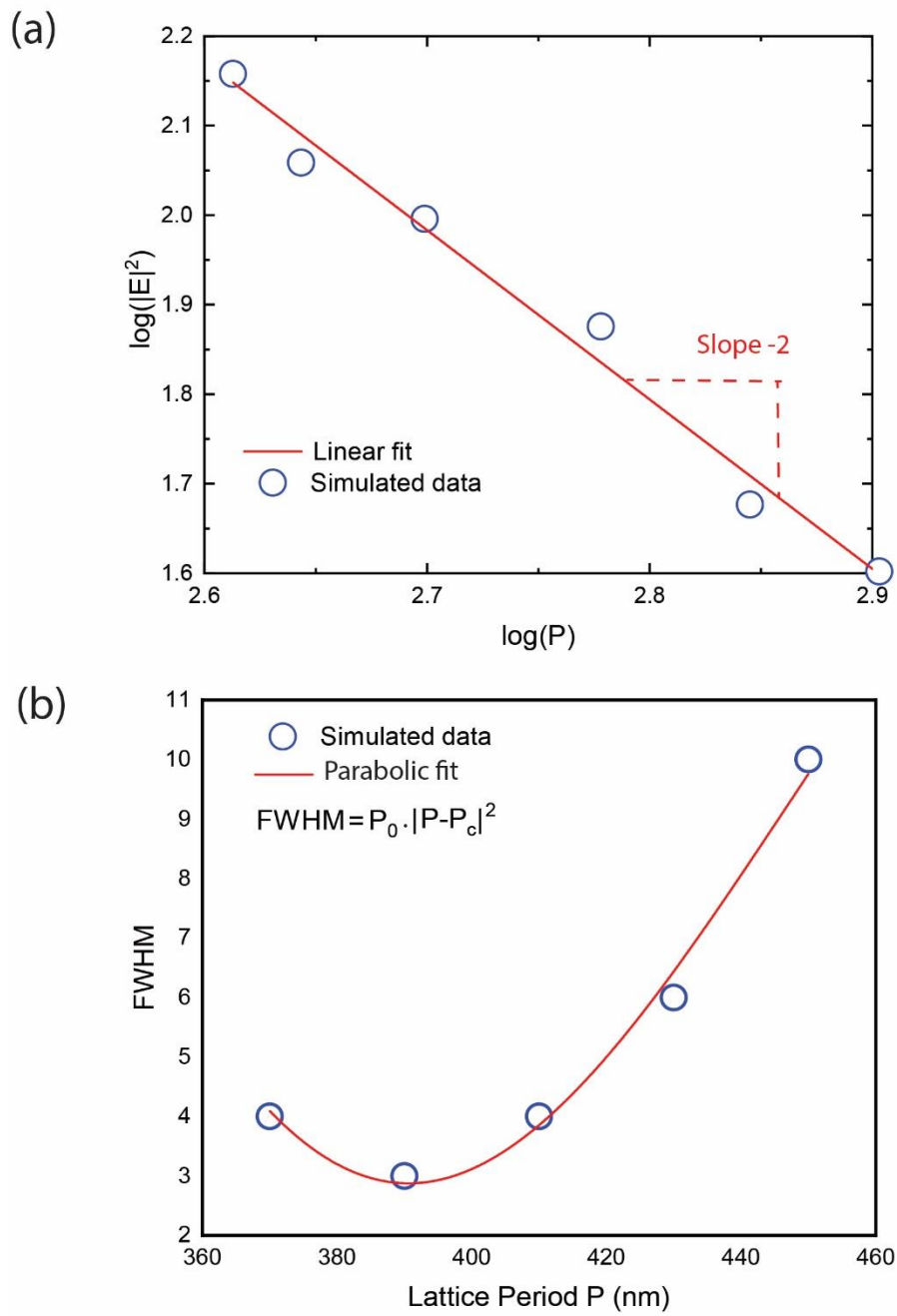


Figure S.I.12. (a) Quadratic dependency of electric field Intensity (E) on lattice period (b) Plot of Full Width Half-Maximum (FWHM) with lattice period showing the Minimum FWHM (corresponding to maximum Q.F.) with lattice period (P).

8. SH-signal 4th Power dependency with lattice period

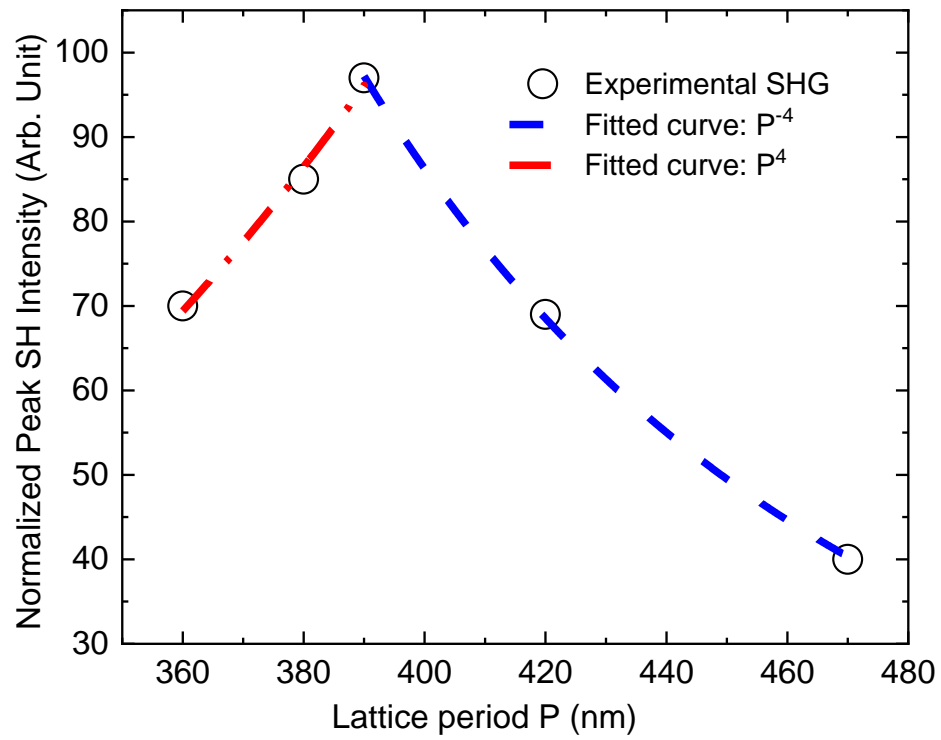


Figure S.I.13. Plot illustrating the 4th power dependency of SH intensity as a function of lattice period (P). The SH intensity is seen to reach maximum at the critical lattice period attributed to critical coupling.

9. Electric field component distribution

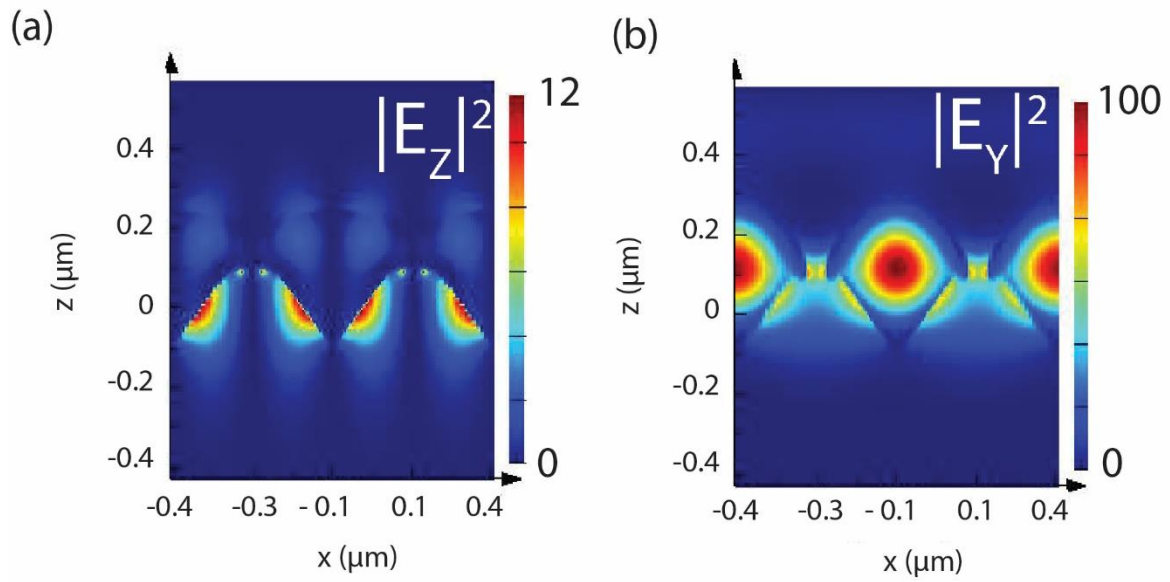


Figure S.I.14. Electric Field component distribution (a) in z -direction showing near 10 times field intensity enhancement in the z -direction. (b) 100 times enhancement in the y direction.